scientific reports

Check for updates

OPEN

Response of erosive rainfall thresholds on Loess slopes to land cover and rainfall intensity

Zimiao He[1], Gangxiang Yuan[1], Zhe Liu[2], Dongyuan Qin[3], Shilong Hao[1]✉, Lu Zhang[1], Peiqing Xiao[4], Ran Wei[1], Haoqiang Tong[1], Huanheng Dou[1] & Yinghong Guo[1]

Rainfall events of sufficient intensity can trigger soil erosion on loess hillslopes. Determining the actual threshold of erosive rainfall events is essential for reducing the workload of soil erosion forecasting and for providing scientific guidance for soil erosion prevention. Based on long-term field observations from runoff plots in representative regions of the Loess Plateau, including Suide, Xifeng, and Tianshui, this study applied an improved regression analysis method to identify rainfall thresholds for soil erosion under different erosion intensities. The variation of rainfall thresholds with rainfall intensity was further examined, and a nonlinear regression approach was used to develop predictive models of rainfall thresholds for soil erosion under different land cover conditions. Rainfall thresholds for slope soil erosion under different land cover types decrease exponentially with increasing rainfall intensity. Influenced by soil texture, rainfall thresholds for soil erosion on woodland, grassland, and bare slopes declined as soil texture became finer, while the rate of decline slowed with increasing rainfall intensity. Soil texture, land cover type, and rainfall characteristics exert significant influences on the effectiveness of vegetation in controlling runoff and soil erosion. These findings provide valuable insights into soil erosion prediction and serve as a reference for soil and water conservation planning.

Keywords Soil erosion, Rainfall threshold model, Slope, Sub-rainfall event, Land cover type

Soil erosion is one of the most severe ecological and environmental challenges worldwide[1–3], and rainfall characteristics are closely linked to both the magnitude and spatial patterns of soil erosion. However, not all rainfall events trigger erosion; only those capable of generating sufficient runoff with sediment transport capacity are considered erosive[4]. Consequently, identifying erosive rainfall remains a central focus and challenge in soil erosion research[5,6]. The Revised Universal Soil Loss Equation (RUSLE) is a widely accepted empirical model for soil erosion assessment[7]. Thresholds of erosive factors represent a major source of uncertainty in RUSLE predictions, while site-specific erosive rainfall thresholds can effectively reduce model uncertainty[8]. Moreover, establishing threshold criteria for erosive rainfall can simplify calculations in practice, enhance the efficiency of identifying erosive rainfall events, and thus improve the assessment of rainfall-induced erosion hazards in specific regions. Therefore, the determination of erosive rainfall thresholds has long been a research priority[9,10].

Numerous scholars have extensively investigated erosive rainfall thresholds[11–13]. Among these, one of the most influential standards was proposed by Wischmeier et al.[14], who defined erosive rainfall in the Universal Soil Loss Equation (USLE) as events with a total rainfall depth of ≥ 12.7 mm, or with a 15-min rainfall depth exceeding 6.4 mm. Wang and Jiao[15] summarized erosive rainfall standards across different regions of China and concluded that a threshold of 10 mm is commonly adopted nationwide. Currently, three main approaches are employed to determine erosive rainfall thresholds: (i) frequency analysis, where cumulative frequency curves of selected rainfall characteristics are plotted, and characteristic values corresponding to cumulative frequencies such as 80%[4,16,15] or 90%[17] are taken as thresholds. Using this approach, Chinese scholars have established erosive rainfall thresholds for the Loess Plateau, northeast Yunnan, northern Jiangxi red-soil region, and purple hill regions, reported as 10 mm, 9.2 mm, 11.2 mm, and 11.3 mm, respectively[4,16–19]. However, this method is subject to considerable subjectivity since frequency parameters are artificially defined[15]. (ii) Rainfall erosivity deviation coefficient method, which involves ranking all rainfall events by erosivity from largest to smallest, then cumulatively summing erosivity values. The characteristic rainfall corresponding to the point at which cumulative erosivity approaches the total erosivity of all erosive rainfall events is defined as the threshold[20]. This method

[1]College of Surveying and Geo-Informatics, North China University of Water Resources and Electric Power, Zhengzhou 450000, China. [2]China South-to-North Water Diversion Corporation, Central Plains Regional Headquarters, Zhengzhou 450000, China. [3]Hydrochina Beijing Engineering Corporation Limited, Beijing 100000, China. [4]Yellow River Institute of Hydraulic Research, Zhengzhou 450000, China. ✉email: haoshilong24@163.com

has been applied to establish erosive rainfall depth and intensity thresholds for regions including the Longdong Loess Plateau, Zizhou in northern Shaanxi, Beijing, and karst areas[21–24]. Although this method incorporates erosive dynamic factors, the determination of the threshold still relies on an empirical "approximate point" on the cumulative curve, which limits its objectivity and precision. (iii) Regression analysis method, which uses selected rainfall characteristics as independent variables and runoff depth as the dependent variable to construct linear regression equations, where the intercept on the x-axis represents the erosive rainfall threshold. Li et al.[25] applied this method to calculate erosive rainfall thresholds for nine types of artificial catchments. Huang et al.[26] applied this method to calculate slope-scale erosive rainfall thresholds under four underlying surface conditions and further developed a multiparameter nonlinear erosive rainfall threshold model. In contrast, the regression analysis method is more objective, as the erosive rainfall threshold is derived directly from the statistical relationships in the observed data, without relying on subjectively defined empirical parameters. This method has a clear mechanistic basis, as it establishes a quantitative relationship between rainfall characteristics and runoff depth, thereby providing the threshold with a more explicit hydrodynamic interpretation. Moreover, the approach is highly flexible, allowing both the construction of linear models to obtain single-parameter thresholds and the further development of multi-parameter nonlinear models to more comprehensively capture the influence of underlying surface conditions on the critical processes governing erosion initiation.

The erosive rainfall threshold is influenced by multiple factors, including geomorphology, soil type, vegetation cover, land use, slope gradient, and rainfall intensity. A study revealed distinct differences in erosive rainfall thresholds between karst and non-karst slopes, with values ranging from 35.4 to 45.6 mm for karst slopes and from 11.8 to 18.8 mm for non-karst slopes[27]. Wang et al.[28] conducted experiments in Fangshan District, Beijing, across five typical soil types representing China's secondary water erosion regions. The results showed that erosive rainfall thresholds were highest for black soil and cinnamon soil (both 10.0 mm), followed by loess soil (9.5 mm), while purple soil and red soil exhibited relatively lower thresholds of 5.4 mm and 6.1 mm, respectively. A long-term study (2006–2022) in the karst yellow soil region, based on 10 experimental stations and 69 plots, further indicated that erosive rainfall thresholds varied across land-use types: 12.66 mm for forest, 10.57 mm for grassland, 9.94 mm for cropland, and 8.93 mm for fallow land. Moreover, croplands with slopes of 13°, 15°, 20°, 23°, and 25° exhibited thresholds of 10.41 mm, 10.28 mm, 9.66 mm, 9.52 mm, and 9.15 mm, respectively[11]. In addition, rainfall characteristics such as intensity exert significant control over erosive rainfall thresholds[29]. At present, thresholds are often defined either as a fixed rainfall depth or as a fixed rainfall intensity. However, laboratory simulations have demonstrated substantial variations in rainfall depth thresholds under different rainfall intensities[30]. This suggests that the variability of erosive rainfall thresholds across rainfall intensities is also an important aspect warranting further investigation.

Since 1999, large-scale ecological restoration programs such as the Grain for Green Program (GFGP) and the Three-North Shelterbelt Forest Program (TNSFP) have contributed to mitigating soil erosion[31,32]. However, soil erosion remains a persistent threat to ecosystem recovery in China[33]. To improve the efficiency of soil erosion monitoring and control, the Ministry of Water Resources[34] classified hydraulic erosion intensity into five grades. Due to the distinct topography and climatic conditions across regions, significant spatial heterogeneity exists in soil erosion. Among these, the Loess Plateau in Northwest China represents one of the most severely eroded landscapes worldwide and has long been a focal area for soil erosion research. Nevertheless, limited attention has been given to the variability of erosive rainfall thresholds under different rainfall intensities. Therefore, this study utilizes long-term runoff plot observations from three representative monitoring stations on the Loess Plateau, applying an improved regression analysis to examine how erosive rainfall thresholds vary with rainfall intensity. Furthermore, a nonlinear regression approach is employed to develop predictive models of erosive rainfall thresholds under different land cover types. The results aim to provide scientific support for regional soil erosion prediction and soil and water conservation planning.

Materials and methods

Overview of the study area

The Loess Plateau is recognized as one of the most severely eroded regions worldwide. Soil erosion in this area results from the combined effects of rainfall, runoff, and soil properties. Li et al.[35] reported that the soils of the Loess Plateau exhibit both consistency in particle composition[36] and distinct zonal distribution. The consistency is reflected in the high proportion of silt particles (0.05–0.001 mm), which generally account for 60–75% of the total soil content, with limited variation across different subregions. Among these, coarse silt particles (0.05–0.01 mm) contribute approximately 50%. The zonal distribution is characterized by a gradual fining of loess particles from northwest to southeast, most evident in the changes of sand and clay fractions. Specifically, Suide soils are classified as sandy loam, whereas Tianshui and Xifeng soils are predominantly clay loam.

Data sources

The field observation data were obtained from soil and water conservation monitoring stations established by the Yellow River Conservancy Commission in Suide, Xifeng, and Tianshui (Fig. 1). The rainfall data used in this study were obtained entirely from field observations based on individual natural rainfall events. In Suide, the runoff plots are located at the Xindian Gully and Yejia Slope experimental fields, representing the first subregion of the hilly–gully area, with a total of 158 plots under different land cover conditions. In Xifeng, the plots are situated in the Nanxiaohe Gully experimental field, characteristic of the Loess Tableland geomorphology, where 62 runoff plots with various land cover types were established over time. In Tianshui, the runoff plots are distributed across the Daliushu Gully and Luoyu Gully experimental fields, representing the third subregion on the hilly–gully area, with 40 plots under different vegetation covers. The detailed information of runoff plots at the three stations is provided in Table 1.

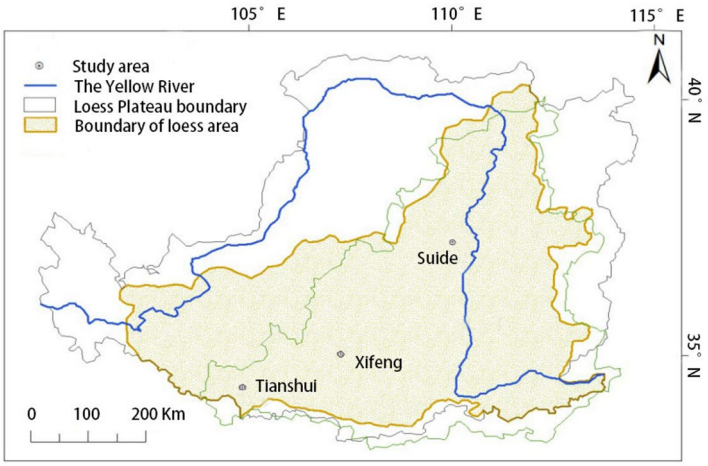

Fig. 1. Schematic diagram of field runoff plot stations—created using ArcGIS (version 10.8, https://www.esri.com/en-us/home).

Observation stations	Cover type	Number of runoff plots (units)	Range of slope (°)	Range of slope length (m)	Observation period (year)
Suide	Forest land	46	7.5 ~ 37	10–50	1956–1963
	Grassland	49	12.5 ~ 40	9.5–54	1955–1963
	Abandoned land	33	4 ~ 51	5–50	1958–1963
	Farmland	30	14 ~ 33	11–32	1955–1963
Xifeng	Forest land	21	17 ~ 48	11–50	1945–1980
	Grassland	8	9 ~ 36	20–50	1957–1980
	Abandoned land	16	8 ~ 28	10–42	1957–1980
	Farmland	17	10 ~ 24	6–20	1955–1980
Tianshui	Forest land	2	28	22	1954–1957
	Grassland	13	7.4 ~ 25	17–23	1954–2010
	Farmland	25	4 ~ 21	20–25	1987–2010

Table 1. Conditions of runoff plots at observation stations.

Analytical methods

The erosive rainfall threshold was determined using the linear regression method adopted by Fink et al.[37–39]. When the linear form is expressed as R = A + B*P = B*(P–C), where R denotes the runoff for a single rainfall event, P the corresponding rainfall amount, and A and B the regression coefficients, then C = –A/B is defined as the erosive rainfall threshold, while B represents the event runoff coefficient. The rainfall–runoff linear model performs well when runoff is substantially greater than zero; however, errors increase when runoff approaches zero, as in the case of natural catchments and natural catchments with weed removal in this study. This limitation can be addressed using Diskin's[37] parameter estimation procedure. Specifically, rainfall observations are first arranged in ascending order, and different candidate threshold rainfall values (P_0) are selected. For events with $P > P_0$, runoff is predicted using R = A + BP, while for events with $P \leq P_0$, runoff is considered negligible. The residual sum of squares between observed and predicted runoff is then calculated, establishing a functional relationship $S = f(P_0)$. The erosive rainfall threshold is defined as the P_0 value corresponding to the minimum residual sum of squares. In addition, rainfall events separated by more than three days were assumed to be unaffected by antecedent rainfall.

For further categorization and analysis, rainfall events were classified according to the Standards for Classification and Gradation of Soil Erosion (SL190-2007) (Table 2)[34]. Within this framework, the variations in event-based runoff depth, rainfall depth, and erosive rainfall thresholds with rainfall intensity were quantified. To distinguish the effect of rainfall intensity on thresholds, rainfall events of the same intensity were retained only if the coefficient of determination between rainfall and runoff exceeded 0.90 ($R^2 \geq 0.90$); otherwise, they were reassigned to a lower intensity class until no runoff was generated. Finally, nonlinear regression analysis was applied to construct predictive models of erosive rainfall thresholds under different land cover conditions.

The geographic data of the Loess Plateau used in this study were obtained from the Loess Plateau Sub-Center of the National Earth System Science Data Center (http://loess.geodata.cn), and spatial mapping was carried out using ArcGIS 10.8 (https://www.esri.com/en-us/home). Data analysis of long-term field observation datasets was performed using IBM SPSS Statistics 27 (https://www.ibm.com), and the final figures were generated using Origin 2022 (https://www.originlab.com).

Land type		Gradient (°)				
		5～8	8～15	15～25	25～35	>35
Non-cultivated land forest and grass coverage (%)	60～75	Mild	Mild	Mild	Moderate	Moderate
	45～60	Mild	Mild	Moderate	Moderate	Strongly
	30～45	Mild	Moderate	Moderate	Strongly	Extremely strong
	< 30	Moderate	Moderate	Strongly	Extremely strong	Violent
Sloping farmland		Mild	Moderate	Strongly	Extremely strong	Violent

Table 2. Classification criteria for areal erosion.

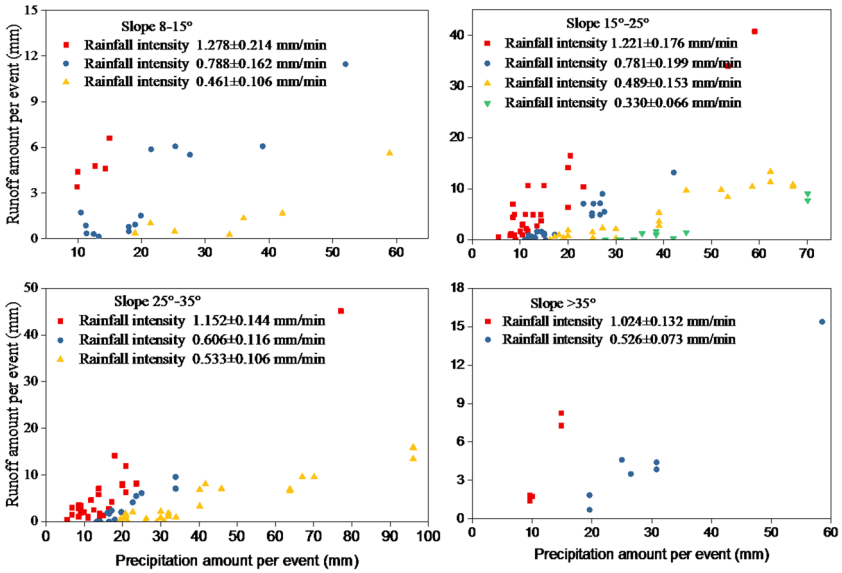

Fig. 2. Trends of erosive rainfall thresholds with mean rainfall intensity on farmland slopes.

Results

Rainfall thresholds for soil erosion under different land cover types

Rainfall thresholds for soil erosion on farmland slopes

In the experiment, the main crops in Suide farmland were sorghum and cowpea. The four slope classes of 8°–15°, 15°–25°, 25°–35°, and > 35° corresponded to moderate, strong, very strong, and severe erosion intensity grades, respectively, according to the Standards for Classification and Gradation of Soil Erosion (SL190-2007). In Xifeng, millet and broomcorn millet were the dominant crops, and the two slope classes of 8°–15° and 15°–25° were classified as moderate and strong erosion intensities, respectively. In Tianshui, the main crop was wheat, and the three slope classes of 5°–8°, 8°–15°, and 15°–25° were categorized as slight, moderate, and strong erosion intensities, respectively.

Taking Suide as an example, scatterplots of event runoff depth versus rainfall amount under different erosion grades are shown in Fig. 2, with regression results summarized in Table 3. The results indicate a strong linear relationship between event rainfall and runoff across varying rainfall intensities. For farmland in Suide, the erosive rainfall thresholds (ERT) under four slope classes (8°–15°, 15°–25°, 25°–35°, > 35°) were 1.3, 10.0, 20.9, 5.5, 11.5, 18.4, 30.6, 7.1, 13.0, 20.7, 8.5, and 14.4 mm. In Xifeng, farmland with two slope classes (8°–15°, 15°–25°) exhibited erosive rainfall thresholds (ERT) of 2.9, 4.2, 18.0, 30.8, 3.6, 8.8, 11.0, and 13.0 mm under different rainfall intensities. For farmland in Tianshui, the erosive rainfall thresholds (ERT) under three slope classes (5°–8°, 8°–15°, 15°–25°) were 3.9, 14.6, 4.5, 14.3, 3.1, and 4.6 mm, respectively.

A regression analysis was conducted between erosive rainfall thresholds and mean rainfall intensity (i.e., the mean of the maximum rainfall intensity for each rainfall event). For Suide, the relationships under severe and extremely severe erosion grades were expressed as $y = 60.591e^{-2.268x}$ ($R^2 = 0.92$, $n = 12$), while for Xifeng, the relationships under intense and moderate erosion grades were expressed as $y = 54.844e^{-2.14x}$ ($R^2 = 0.97$, $n = 8$). A comparison of the two regions indicates that the variation trends of erosive rainfall thresholds with mean rainfall intensity in farmland slopes of Xifeng and Suide are generally consistent.

The relationship between erosive rainfall thresholds and mean rainfall intensity under different erosion intensity classes in Suide and Xifeng was fitted to an exponential function, expressed as $y = 59.986e^{-1.888x}$ ($R^2 = 0.65$, $n = 20$). When combining Suide, Xifeng, and Tianshui, the relationship was expressed as $y = 27.693e^{-1.35x}$ ($R^2 = 0.43$, $n = 27$). These results indicate that in Suide and Xifeng, the relationship between erosive rainfall thresholds and mean rainfall intensity can still be described by an exponential function, although the fitting

Observation stations	Erosion grade	Slope (°)	Rainfall intensity (mm/min)	*n*	Fitting equation	R^2	ERT (mm)
Suide	Moderate	8 ~ 15	1.278 ± 0.214	6	y = 0.426x- 0.5378	0.91	1.3
			0.788 ± 0.162	14	y = 0.264x – 2.628	0.92	10.0
			0.461 ± 0.106	8	y = 0.119x – 2.479	0.91	20.9
	Intense	15 ~ 25	1.221 ± 0.176	36	y = 0.737x – 4.017	0.90	5.5
			0.781 ± 0.199	30	y = 0.426x – 4.899	0.92	11.5
			0.489 ± 0.153	28	y = 0.246x – 4.506	0.91	18.4
			0.330 ± 0.066	14	y = 0.195x – 5.949	0.91	30.6
	Extremely intense	25 ~ 35	1.152 ± 0.144	36	y = 0.624x – 4.448	0.90	7.1
			0.606 ± 0.116	22	y = 0.393x – 5.112	0.91	13.0
			0.533 ± 0.106	43	y = 0.194x – 4.022	0.90	20.7
	Severe	> 35	1.024 ± 0.132	6	y = 0.614x – 5.247	0.98	8.5
			0.526 ± 0.073	11	y = 0.326x – 4.681	0.96	14.4
Xifeng	Moderate	8 ~ 15	1.370 ± 0.257	55	y = 0.615x – 1.786	0.90	2.9
			1.090 ± 0.304	48	y = 0.507x – 2.137	0.92	4.2
			0.565 ± 0.109	36	y = 0.181x – 3.246	0.91	18.0
			0.264 ± 0.046	20	y = 0.076x – 2.347	0.90	30.8
	Intense	15 ~ 25	1.307 ± 0.242	44	y = 0.761x – 2.707	0.90	3.6
			0.938 ± 0.220	57	y = 0.463x – 4.073	0.92	8.8
			0.783 ± 0.169	19	y = 0.258x – 2.847	0.90	11.0
			0.599 ± 0.203	31	y = 0.211x – 2.741	0.90	13.0
Tianshui	Mild	5 ~ 8	0.590 ± 0.125	31	y = 0.426x – 1.681	0.91	3.9
			0.409 ± 0.114	20	y = 0.390x – 5.669	0.94	14.6
	Moderate	8 ~ 15	0.615 ± 0.137	44	y = 0.475x – 2.113	0.92	4.5
			0.401 ± 0.096	27	y = 0.228x – 3.268	0.91	14.3
	Intense	15 ~ 25	0.461 ± 0.105	14	y = 0.468x – 1.524	0.90	3.1
			0.341 ± 0.102	21	y = 0.234x – 1.397	0.91	4.6

Table 3. Relationships between erosive rainfall thresholds and rainfall intensity under different erosion intensity classes on farmland slopes across the study regions.

accuracy decreases. In contrast, the relationship in Tianshui differs markedly from that in Suide and Xifeng. Moreover, it can be observed that with the southwestward shift of the study area, the rate of decline in erosive rainfall thresholds with increasing mean rainfall intensity becomes less pronounced.

Rainfall thresholds for soil erosion on forest land slopes

In the different study areas, the dominant forest land species was Robinia pseudoacacia. In Suide, vegetation cover was categorized into four levels: <30%, 30%–45%, 45%–60%, and > 60%. The corresponding slope classes were 25°–35°, 25°–35° & 8°–25°, 15°–35°, and > 25°, which were classified as extremely severe, severe & moderate, moderate, and moderate erosion intensity levels, respectively. In Xifeng, vegetation cover was grouped into three levels: 30%–45%, 45%–60%, and > 60%. The associated slope classes were 25°–35°, 15°–35°, and > 25°, corresponding to severe, moderate, and moderate erosion intensity levels, respectively. In Tianshui, vegetation cover ranged between 61% and 85%, with slopes greater than 43°, which were classified as moderate erosion intensity.

Taking Suide as an example, scatter plots of event runoff depth versus event rainfall depth under different erosion severity classes are presented in Fig. 3. Across different rainfall intensities, event runoff depth and event rainfall depth exhibited strong linear relationships, with the regression results summarized in Table 4. In Suide, the erosive rainfall thresholds (ERT) for forest land under four vegetation cover and slope classes were 8.0, 17.7, 30.3, 8.1, 9.4, 19.1, 36.7, 4.0, 13.8, 24.8, 37.3, 8.9, 15.4, 25.9, and 38.5 mm across different rainfall intensities. In Xifeng, the erosive rainfall thresholds for forest land under three vegetation cover and slope classes were 4.4, 16.8, 37.0, 19.2, 32.2, 8.7, 20.9, and 34.1 mm. In Tianshui, the erosive rainfall thresholds for forest land under one vegetation cover and slope class were 6.4, 15.2, and 24.2 mm.

By fitting the relationship between erosive rainfall thresholds and mean rainfall intensity under different erosion severity classes, it was found that, for the moderate erosion class, the relationships for Xifeng and Suide were expressed as $y = 48.434e^{-1.097x}$ ($R^2 = 0.94$, $n = 5$) and $y = 88.885e^{-2.19x}$ ($R^2 = 0.97$, $n = 9$), respectively. When combining the moderate and strong erosion classes, the corresponding relationships were $y = 50.019e^{-1.367x}$ ($R^2 = 0.86$, $n = 8$) for Xifeng and $y = 81.482e^{-2.121x}$ ($R^2 = 0.96$, $n = 12$) for Suide. A comparison of the trends revealed that, under the same erosion severity class, the erosive rainfall thresholds in Suide decreased more rapidly with increasing mean rainfall intensity than those in Xifeng.

By fitting the relationship between erosive rainfall thresholds and mean rainfall intensity for Suide and Xifeng, the function was expressed as $y = 58.943e^{-1.668x}$ ($R^2 = 0.84$, $n = 3$). When incorporating data from Suide, Xifeng, and Tianshui, the fitted function was $y = 47.227e^{-1.487x}$ ($R^2 = 0.67$, $n = 26$). These results indicate that the

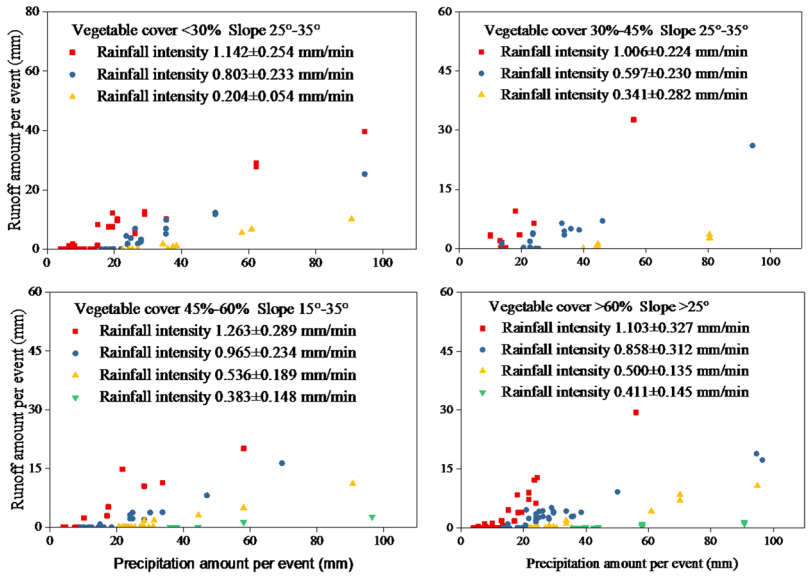

Fig. 3. Trends of erosive rainfall thresholds with mean rainfall intensity on forest land slopes.

Observation stations	Erosion grade	Vegetation cover (%)	Slope (°)	Rainfall intensity (mm/min)	*n*	Fitting equation	R^2	ERT (mm)
Suide	Extremely intense	<30	25~35	1.142±0.254	61	y=0.488x−3.899	0.94	8.0
				0.803±0.233	35	y=0.345x−6.096	0.94	17.7
				0.204±0.054	17	y=0.171x−5.164	0.90	30.3
	Moderate	30–45	8~25	1.116±0.247	12	y=0.077x−0.626	0.94	8.1
	Intense	30–45	25~35	1.006±0.224	11	y=0.664x−6.242	0.90	9.4
				0.597±0.230	19	y=0.323x−6.152	0.91	19.1
				0.341±0.082	8	y=0.067x−2.454	0.91	36.7
	Moderate	45–60	15~35	1.263±0.289	13	y=0.403x−1.615	0.90	4.0
				0.965±0.234	24	y=0.259x−3.561	0.93	13.8
				0.536±0.189	25	y=0.159x−3.928	0.94	24.8
				0.383±0.148	7	y=0.046x−1.707	0.97	37.3
	Moderate	60>	>25	1.103±0.327	57	y=0.564x−5.039	0.90	8.9
				0.858±0.312	63	y=0.226x−3.477	0.93	15.4
				0.500±0.135	30	y=0.155x−4.007	0.95	25.9
				0.411±0.145	25	y=0.027x−1.021	0.90	38.5
Xifeng	Intense	30–45	25~35	1.029±0.386	24	y=0.436x−1.916	0.90	4.4
				0.897±0.217	28	y=0.254x−4.273	0.92	16.8
				0.225±0.091	29	y=0.175x−6.490	0.91	37.0
	Moderate	45–60	15~35	0.893±0.244	9	y=0.521x−10.015	0.90	19.2
				0.304±0.097	8	y=0.095x−3.056	0.91	32.2
	Moderate	60>	25>	1.408±0.155	34	y=0.842x−7.339	0.91	8.7
				0.979±0.122	22	y=0.200x−4.178	0.90	20.9
				0.283±0.089	11	y=0.108x−3.677	0.90	34.1
Tianshui	Moderate	60>	25>	0.704±0.190	15	y=0.218x−1.398	0.90	6.4
				0.294±0.103	12	y=0.163x−2.478	0.91	15.2
				0.228±0.009	5	y=0.054x−1.308	0.93	24.2

Table 4. Relationships between erosive rainfall thresholds and rainfall intensity under different erosion intensity classes on forest land slopes across the study regions.

relationship between ERTs and mean rainfall intensity across regions and erosion severity classes can still be described using an exponential function, although the fitting accuracy gradually decreases. Moreover, it was observed that with the southwestward shift of the study area (accompanied by a finer soil texture), the erosive rainfall thresholds on forested slopes progressively decreased, and the rate of decline with increasing rainfall intensity became less pronounced.

Rainfall thresholds for soil erosion on grassland slopes

In the Suide region, the main pasture species included Medicago sativa (alfalfa), Melilotus spp., and Bothriochloa ischaemum. Vegetation cover was categorized into four classes: <30%, 30–45%, 45–60%, and >60%. The corresponding slope gradients were 25–35°, 8–25°, 15–35°, and >25°, respectively, which fall into the categories of extremely severe, moderate, moderate, and moderate erosion intensity according to the Standards for Classification and Gradation of Soil Erosion (SL190-2007). In the Xifeng region, the main pasture species were Melilotus spp. and Medicago sativa. Vegetation cover was divided into two classes, 30–45% and 45–60%, with slope gradients of 15–25° and 5–15°, corresponding to severe and slight erosion intensity, respectively. In the Tianshui region, the pastures mainly consisted of Medicago sativa, Coronilla varia, Onobrychis viciifolia, and Bothriochloa ischaemum. Vegetation cover ranged from 60% to 95%, and slopes varied from 7.4° to 25°, corresponding to slight erosion intensity according to the same classification standard.

Taking the Suide region as an example, scatterplots of event-based runoff against rainfall under different erosion intensity classes are shown in Fig. 4. Across different rainfall intensities, event runoff exhibited a strong linear relationship with event rainfall, with regression results summarized in Table 5. In Suide, the erosive rainfall thresholds (ERT) of pastureland under five cover–slope classes were 5.1, 13.4, 30.4, 7.5, 13.2, 15.9, 40.2, 11.3, 21.7, 27.7, 5.5, 10.0, 19.4, 26.6, 3.0, 9.8, 15.8, and 23.2 mm across different rainfall intensities. In Xifeng, the erosive rainfall thresholds for pastureland under two cover–slope classes were 7.6, 17.1, 22.5, 39.9, and 10.8 mm. In Tianshui, the erosive rainfall thresholds for pastureland under two cover–slope classes were 4.7, 16.0, and 15.5 mm.

By fitting the relationship between erosive rainfall thresholds and rainfall intensity under different erosion intensity classes, the functional expressions for Xifeng (severe and slight erosion) and Suide (very severe, severe, and moderate erosion) were obtained as $y = 56.026e^{-1.636x}$ ($R^2 = 0.93$, $n = 5$), $y = 71.142e^{-2.222x}$ ($R^2 = 0.79$, $n = 18$), respectively. A comparison of the trends indicates that the erosive rainfall threshold in Suide declines more rapidly with increasing mean rainfall intensity than in Xifeng.

The relationship between erosive rainfall thresholds and mean rainfall intensity under different erosion intensity classes for Suide and Xifeng was fitted as $y = 64.596e^{-2.034x}$ ($R^2 = 0.83$, $n = 23$), while for Suide, Xifeng, and Tianshui it was fitted as $y = 53.56e^{-1.889x}$ ($R^2 = 0.72$, $n = 26$). These results indicate that the relationship between erosive rainfall thresholds and mean rainfall intensity under different erosion intensity classes across regions can still be described by an exponential function, although the fitting accuracy gradually decreases. Moreover, on grassland slopes, the erosive rainfall threshold gradually decreases with finer soil texture, and the rate of decline slows with increasing rainfall intensity.

Rainfall thresholds for soil erosion on abandoned land slopes

In Suide, the vegetation in the abandoned land mainly consists of Artemisia scoparia, Stipa bungeana, Artemisia capillaris, Setaria viridis, and other species. Vegetation cover is categorized into two levels, <30% and 30%–45%, with corresponding slope gradients all >35°, classified as severe and extremely severe erosion intensity according to the "Soil Erosion Classification and Grading Standard." In Xifeng, the abandoned land are dominated by

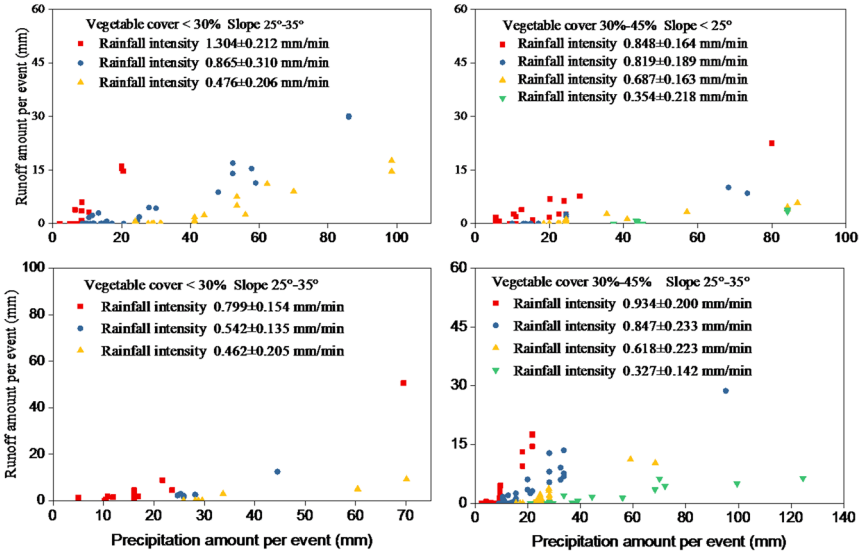

Fig. 4. Trends of erosive rainfall thresholds with mean rainfall intensity on grassland slopes.

Observation stations	Erosion grade	Vegetation cover (%)	Slope (°)	Rainfall intensity (mm/min)	*n*	Fitting equation	R^2	ERT (mm)
Suide	Extremely intense	< 30	25 ~ 35	1.304 ± 0.212	21	y = 0.964x − 4.875	0.90	5.1
				0.865 ± 0.310	44	y = 0.361x − 4.840	0.93	13.4
				0.476 ± 0.206	24	y = 0.231x − 7.007	0.90	30.4
	Moderate	30–45	8 ~ 25	0.848 ± 0.164	25	y = 0.304x − 2.271	0.90	7.5
				0.819 ± 0.189	17	y = 0.162x − 2.128	0.97	13.2
				0.687 ± 0.163	14	y = 0.071x − 1.128	0.90	15.9
				0.354 ± 0.218	11	y = 0.082x − 3.284	0.93	40.2
	Moderate	45–60	15 ~ 35	0.799 ± 0.154	13	y = 0.822x − 9.244	0.95	11.3
				0.542 ± 0.135	6	y = 0.537x − 11.652	0.97	21.7
				0.462 ± 0.205	10	y = 0.194x − 5.340	0.93	27.7
	Moderate	60>	25>	1.201 ± 0.201	18	y = 0.933x − 5.101	0.91	5.5
				1.008 ± 0.317	34	y = 0.354x − 3.544	0.90	10.0
				0.681 ± 0.378	22	y = 0.236x − 4.587	0.91	19.4
				0.598 ± 0.281	23	y = 0.076x − 2.021	0.90	26.6
	Intense	30–45	25 ~ 35	0.934 ± 0.200	15	y = 0.792x − 2.384	0.91	3.0
				0.847 ± 0.233	48	y = 0.618x − 6.036	0.95	9.8
				0.618 ± 0.223	30	y = 0.348x − 5.513	0.93	15.8
				0.327 ± 0.142	17	y = 0.282x − 6.540	0.98	23.2
Xifeng	Intense	30%<	15 ~ 25	1.154 ± 0.234	27	y = 0.667x − 5.100	0.91	7.6
				0.864 ± 0.172	14	y = 0.479x − 8.195	0.94	17.1
				0.439 ± 0.103	18	y = 0.115x − 2.593	0.90	22.5
				0.258 ± 0.055	13	y = 0.085x − 3.386	0.90	39.9
	Mild	45–60	5 ~ 15	1.004 ± 0.290	11	y = 0.002x − 0.018	0.91	10.8
Tianshui	Mild	60>	5 ~ 15	0.671 ± 0.208	21	y = 0.472x − 2.229	0.90	4.7
				0.508 ± 0.178	29	y = 0.298x − 4.767	0.90	16.0
			15 ~ 25	0.442 ± 0.207	65	y = 0.262x − 4.060	0.91	15.5

Table 5. Relationships between erosive rainfall thresholds and rainfall intensity under different erosion intensity classes on grassland slopes across the study regions.

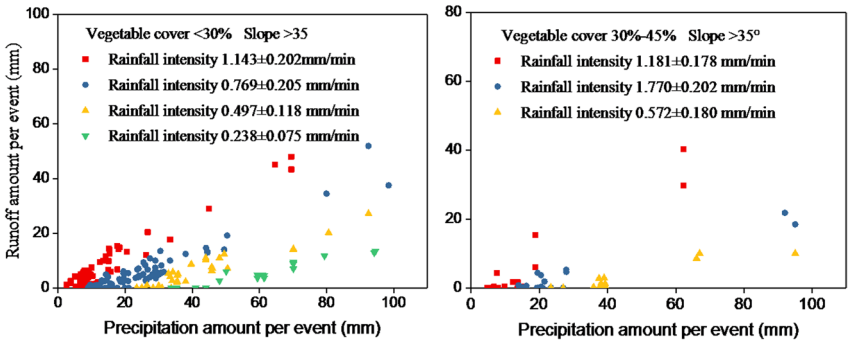

Fig. 5. Trends of erosive rainfall thresholds with mean rainfall intensity on abandoned land slopes.

Artemisia, Bothriochloa ischaemum, Agropyron cristatum, and Cleistogenes, with three vegetation cover levels: 30%–45%, 45%–60%, and > 60%, all with slope gradients of 25°–35°, corresponding to strong, moderate, and moderate erosion intensity levels, respectively, based on the same standard.

Taking Suide as an example, the scatter plots of event-based runoff versus event rainfall under different erosion intensity levels are shown in Fig. 5. Across varying rainfall intensities, event runoff exhibits a strong linear relationship with event rainfall, with the fitting results detailed in Table 6. In Suide, the erosion rainfall thresholds (ERT) for abandoned land under two vegetation cover and slope classes are 3.6, 13.0, 25.6, 37.2, 7.9, 16.1, and 29.6 mm. In Xifeng, the erosive rainfall thresholds for abandoned land under three vegetation cover and slope classes are 5.3, 13.1, 25.1, 5.8, 23.9, 31.6, 5.7, 17.1, and 29.9 mm.

Fitting the erosion rainfall thresholds against rainfall intensity under different erosion levels, the relationships for Xifeng under strong and moderate erosion intensity and for Suide under severe and extreme erosion intensity are expressed as $y = 78.32e^{-2.482x}$ ($R^2 = 0.76$, $n = 9$) and $y = 77.973e^{-2.235x}$ ($R^2 = 0.88$, $n = 7$), respectively. A

Observation stations	Erosion grade	Vegetation cover (%)	Slope (°)	Rainfall intensity (mm/min)	*n*	Fitting equation	R^2	ERT (mm)
Suide	Severe	< 30	> 35	1.143 ± 0.202	65	y = 0.705x – 2.565	0.90	3.6
				0.769 ± 0.205	93	y = 0.486x – 6.292	0.90	13.0
				0.497 ± 0.118	37	y = 0.378x – 9.696	0.91	25.6
				0.238 ± 0.075	19	y = 0.237x – 8.813	0.91	37.2
	Extremely intense	30–45	> 35	1.181 ± 0.178	20	y = 0.632x – 4.988	0.90	7.9
				0.770 ± 0.202	22	y = 0.259x – 4.176	0.92	16.1
				0.572 ± 0.180	13	y = 0.185x – 5.485	0.90	29.6
Xifeng	Intense	30–45	25 ~ 35	0.824 ± 0.246	16	y = 0.266x – 1.411	0.91	5.3
				0.687 ± 0.223	18	y = 0.131x – 1.709	0.91	13.1
				0.548 ± 0.200	15	y = 0.064x – 1.604	0.90	25.1
	Moderate	45–60	25 ~ 35	0.777 ± 0.271	30	y = 0.246x – 1.434	0.91	5.8
				0.454 ± 0.133	10	y = 0.196x – 4.692	0.93	23.9
				0.368 ± 0.108	8	y = 0.044x – 4.692	0.90	31.6
	Moderate	60>	25 ~ 35	1.167 ± 0.130	36	y = 0.212x – 1.206	0.95	5.7
				0.845 ± 0.144	29	y = 0.147x – 2.507	0.92	17.1
				0.543 ± 0.088	20	y = 0.113x – 3.362	0.90	29.9

Table 6. Relationships between erosive rainfall thresholds and rainfall intensity under different erosion intensity classes on abandoned land slopes across the study regions.

comparison of the trends indicates that the erosion rainfall thresholds for wasteland slopes in Xifeng and Suide decrease with increasing average rainfall intensity in a nearly consistent manner.

The relationship between erosion rainfall thresholds and mean rainfall intensity for different erosion intensity levels in Suide and Xifeng was fitted using the function $y = 74.809e^{-2.308x}$ ($R^2 = 0.80$, $n = 16$), indicating that the relationship across different regions and erosion intensity levels can still be expressed using an exponential function.

Influence of land cover types on rainfall thresholds for soil erosion

Rainfall thresholds for soil erosion in the suide region

In this study, the linear regression method was used to estimate the slope erosive rainfall thresholds. It was found that in the Suide, under different land cover types, the rainfall thresholds for slope soil erosion decreased exponentially with increasing rainfall intensity.

Slope vegetation cover is a key factor influencing the slope erosive rainfall thresholds. The variation of erosion rainfall thresholds with mean rainfall intensity under different land cover types in Suide is shown in Fig. 6. Here, the fitted curves represent erosive rainfall thresholds across all erosion classes defined in China's "Soil Erosion Classification and Grading Standard" (SL190-2007). The fitted equations for forest land, grassland, abandoned land, and farmland are $y = 68.15e^{-1.907x}$ ($R^2 = 0.83$, $n = 15$), $y = 71.142e^{-2.222x}$ ($R^2 = 0.79$, $n = 18$), $y = 77.973e^{-2.235x}$ ($R^2 = 0.87$, $n = 7$), and $y = 60.248e^{-2.256x}$ ($R^2 = 0.92$, $n = 15$), respectively. Comparison of the fitted coefficients indicates that the rainfall threshold for soil erosion decreases most rapidly on abandoned land, followed by grassland and forest land, while farmland decreases most slowly. Due to these differences in decline rates among land cover types, Fig. 6 shows that for rainfall intensities below 0.4 mm/min, the threshold order is forest land > abandoned land ≈ grassland > farmland; for rainfall intensities above 0.4 mm/min, the order becomes forest > abandoned land > grassland > farmland. The soil erosion rainfall thresholds under different rainfall intensities in Suide are listed in Table 7.

Rainfall thresholds for soil erosion in the Xifeng region

In this study, the erosive rainfall threshold for slope surfaces was determined using the linear regression method. Similarly, it was found that in the Xifeng, the slope erosive rainfall thresholds under different land cover types decreased exponentially with increasing rainfall intensity.

The variation trends of slope erosive rainfall thresholds under different land cover types in Xifeng are shown in Fig. 7. The fitted curves of erosion rainfall thresholds with average rainfall intensity for forest land, grassland, abandoned land, and farmland are expressed as $y = 50.022e^{-1.367x}$ ($R^2 = 0.86$, $n = 8$), $y = 56.026e^{-1.636x}$ ($R^2 = 0.93$, $n = 5$), $y = 78.32e^{-2.482x}$ ($R^2 = 0.76$, $n = 9$), and $y = 82.922e^{-1.776x}$ ($R^2 = 0.83$, $n = 8$), respectively. Comparing the fitted coefficients shows that the erosive rainfall thresholds on farmland decreases most rapidly with increasing rainfall intensity, followed by abandoned land and grassland, while forest land decreases the slowest. Due to the differing rates of decline in erosive rainfall thresholds among land cover types, Fig. 7 shows that for rainfall intensities below 0.4 mm/min, the trend of soil erosion rainfall thresholds is abandoned land > grassland > forest land > farmland; for rainfall intensities above 0.4 mm/min, the trend is forest land > grassland ≈ abandoned land > farmland. The rainfall thresholds for soil erosion under different rainfall intensities in Xifeng are listed in Table 8.

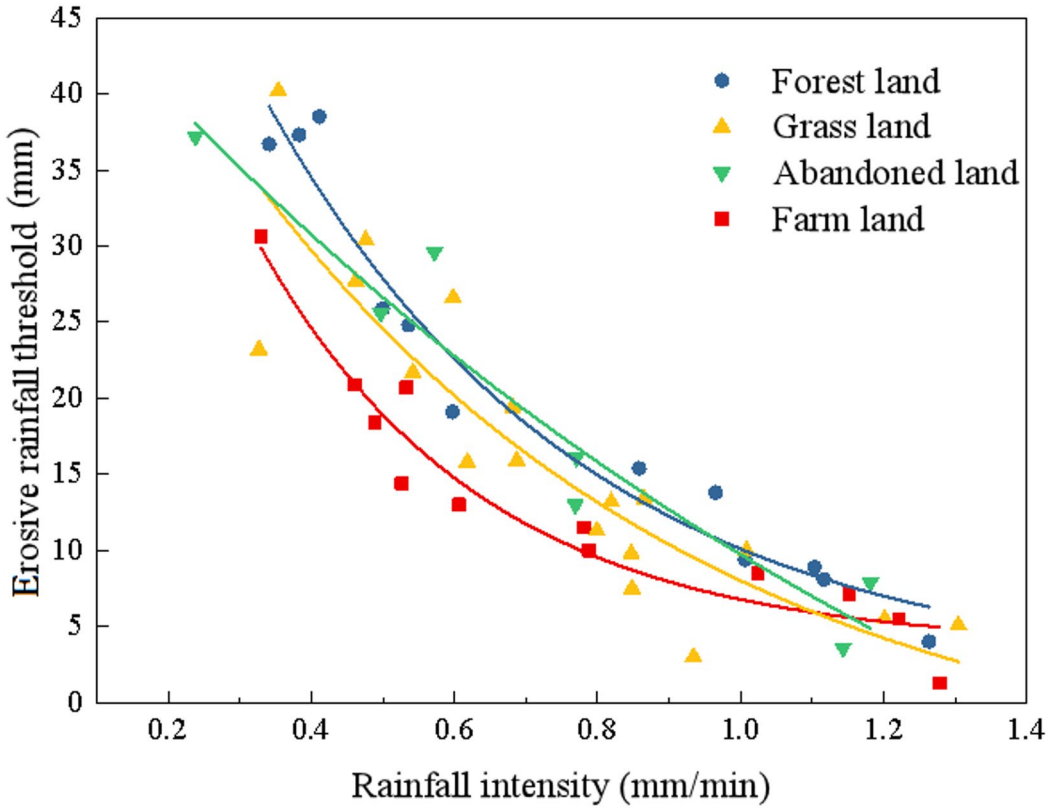

Fig. 6. Variation of erosive rainfall thresholds with mean rainfall intensity under different land cover types in Suide.

	Erosive rainfall threshold (mm)			
Rainfall intensity (mm/min)	Forest land	Grassland	Abandoned land	Farmland
0.2	46.5	45.6	49.9	38.4
0.4	31.8	29.2	31.9	24.4
0.6	21.7	18.8	20.4	15.6
0.8	14.8	12.0	13.0	9.9
1.0	10.1	7.7	8.3	6.3
1.2	6.9	4.9	5.3	4.0

Table 7. Variation of erosive rainfall thresholds with rainfall intensity under different land cover types in Suide.

Discussion

The erosive rainfall thresholds serve as fundamental parameters for studies on slope runoff regulation and soil erosion prediction. In this study, the erosive rainfall thresholds were estimated using a linear regression approach, revealing that the erosive rainfall thresholds decrease exponentially with increasing rainfall intensity under different land cover types. This pattern may be attributed to the loess soil's loose structure and well-developed porosity, which make it highly susceptible to raindrop impact and particle dispersion. Under high-intensity rainfall, the kinetic energy of raindrops can rapidly destroy soil aggregates, causing fine particles to clog pores and form a dense surface crust. This process nonlinearly, and even exponentially, reduces soil infiltration capacity. Once infiltration falls below rainfall intensity, surface water rapidly accumulates, significantly shortening the time to runoff initiation and, consequently, to soil erosion, resulting in an exponential decline of erosive rainfall thresholds with increasing rainfall intensity. Huang et al.[40] analyzed the relationship between individual rainfall events and runoff depth in eight experimental plots (forest + understory shrub-grass) in the Pearl River Basin and found a linear decrease of erosive rainfall thresholds with increasing rainfall intensity, which differs slightly from the present study. The discrepancy may be due to their rainfall intensity classification, where the highest categories were 30–35 mm/h and > 35 mm/h, lacking data on high-intensity rainfall events; under such conditions, slope runoff occurs rapidly, and the decrease in erosive rainfall thresholds with increasing intensity is less pronounced. Overall, on loess slopes, short-duration, high-volume rainfall events can rapidly generate

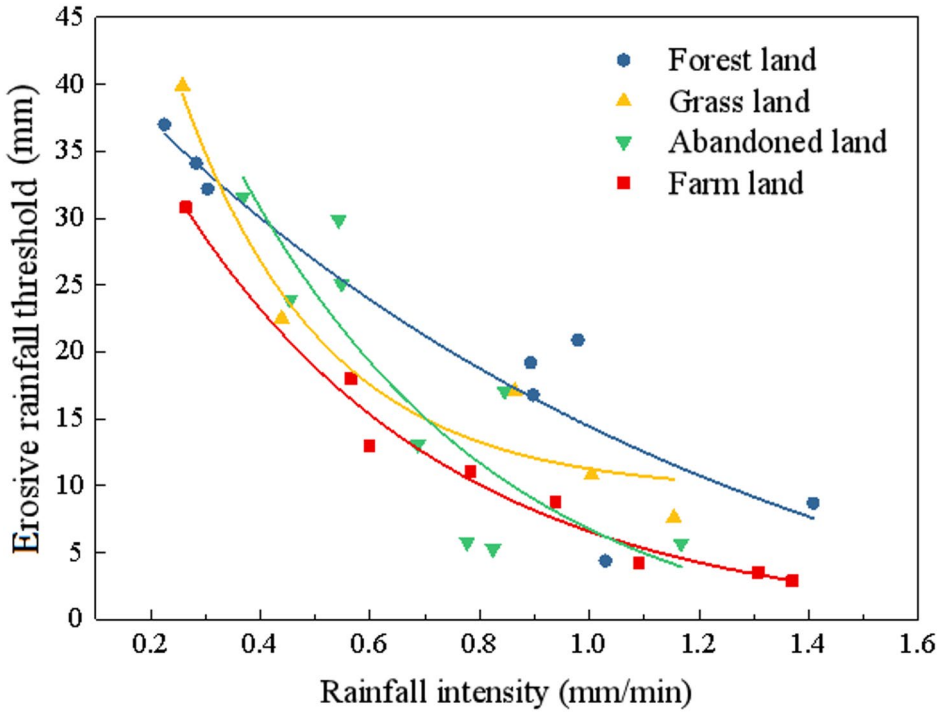

Fig. 7. Variation of erosive rainfall thresholds with mean rainfall intensity under different land cover types in Xifeng.

Rainfall intensity (mm/min)	Erosive rainfall threshold (mm)			
	Forest land	Grassland	Abandoned land	Farmland
0.2	38.1	40.4	47.7	35.1
0.4	29.0	29.1	29.0	22.8
0.6	22.0	21.0	17.7	15.4
0.8	16.8	15.1	10.8	10.2
1.0	12.7	10.9	6.5	6.4
1.2	9.7	7.9	4.0	4.1

Table 8. Variation of erosive rainfall thresholds with rainfall intensity under different land cover types in Xifeng.

surface runoff and enhance sediment transport capacity, causing severe soil erosion. Furthermore, studies have shown that the Revised Universal Soil Loss Equation (RUSLE) tends to overestimate soil erosion under vegetation recovery conditions[8], likely because RUSLE uses fixed erosion thresholds that do not account for variations with vegetation cover or erosion intensity, nor the response of thresholds to rainfall intensity. The predictive models of erosive rainfall thresholds under different land cover types developed in this study can provide useful references for RUSLE-based soil erosion prediction and help reduce its calculation uncertainties.

Slope vegetation cover is a critical factor influencing the slope erosive rainfall thresholds. Vegetation can delay crust formation by intercepting raindrops, increasing surface roughness, and improving soil structure[41,42], thereby raising erosion rainfall thresholds. Different vegetation measures effectively mitigated soil erosion, with the annual mean soil loss ranked as follows: natural vegetation restoration < cropland < bare land[43]. Therefore, different slope cover conditions exhibit varying capacities to increase the slope erosive rainfall thresholds. Wang Wanzhong[4] suggested that the basic erosive rainfall thresholds in the Loess Plateau are: farmland 8.1 mm < artificial grassland 10.9 mm < forest land 14.6 mm, with the required rainfall intensities generally exceeding 0.26 mm/min, 0.32 mm/min, and 0.32 mm/min for the respective land covers (based on average intensity of individual rainfall events). In the present study, at a rainfall intensity of 0.8 mm/min, the slope erosive rainfall thresholds in Suide were: farmland 9.9 mm < grassland 12.0 mm < barren land 13.0 mm < forest land 14.8 mm, and in Xifeng: farmland 10.2 mm < barren land 10.8 mm < grassland 15.1 mm < forest land 16.8 mm. In terms of rainfall amounts, these results are roughly consistent with Wang Wanzhong's findings. Regarding the corresponding rainfall intensities, this study used the mean of the maximum intensities of individual rainfall events, whereas Wang used the mean rainfall intensity, which may explain why the rainfall intensities corresponding to similar thresholds are higher in this study. Differences may also arise from variations in vegetation types, coverage,

slope, and soil texture between the experimental plots in this study and those in Wang's work. Wang et al. reported erosive rainfall thresholds at a single rainfall intensity, whereas this study presents curves of rainfall thresholds for different cover types as a function of rainfall intensity, further improving the precision of threshold estimation. Both this study and previous research[11] indicate that forested slopes have higher soil erosion rainfall thresholds than grassland or farmland. This is likely because soil erosion is primarily driven by surface runoff, and erosion under forest canopies is mitigated by the canopy intercepting rainfall[44], filtering raindrops, and enhancing soil stability through root structures[45,46]. Modeste et al.[47] found that, in non-karst regions, infiltration capacity follows the order: forest land > farmland > bare land; the higher infiltration capacity of forest soils also contributes to their larger erosion rainfall thresholds.

Soil texture is also an important factor influencing runoff generation on slopes. In this study, it was observed that on forest, grassland, and barren slopes, as the study area shifts southwestward (i.e., with increasingly fine-textured soils), the rate of decline in erosive rainfall thresholds with increasing mean rainfall intensity gradually slows. Zhou Peihua and Wang Zhanli[48] reported from farmland plots on clay loess, sandy loess, and loessial soils that soil texture had no significant effect on runoff initiation time, arguing that tillage of farmland masks the role of soil texture. Frequent tillage increases macropores in the topsoil, which may lead to higher erosive rainfall thresholds—likely explaining the relatively large erosive rainfall thresholds for farmland observed in Xifeng. However, quantitatively evaluating the influence of soil properties on the proposed thresholds is not straightforward. For instance, erosive rainfall thresholds generally increase with clay content[49]. Yet, in some cases—such as soils with high exchangeable sodium percentage (ESP) or sodium adsorption ratio (SAR)[13]—clay can behave very differently, reducing soil structural stability and increasing susceptibility to erosion processes.

At the same time, rainfall characteristics vary markedly across regions. de Almeida et al.[50] demonstrated that for rainfall events with equivalent erosive power, differences in rainfall intensity and duration can alter both the onset time of runoff and the runoff volume. Regional variations in rainfall characteristics are therefore one of the key reasons for the differences in erosive rainfall thresholds between Suide and Xifeng. In addition, differences in topography and climatic conditions across regions result in distinct standards for erosive rainfall. Findings from this study, together with previous research, support this perspective. For instance, some scholars define erosive rainfall in the Loess Plateau as events with rainfall amounts greater than 10 mm[18]; in northeastern Heilongjiang, the threshold for soil erosion is 9.8 mm[51]; in the northeastern mountainous regions of Yunnan Province, it is 9.2 mm[19]; whereas in the Poyang Lake Basin, the standard for erosive rainfall is 14 mm[52]. Such erosive rainfall thresholds provide an effective criterion for distinguishing rainfall events capable of generating soil erosion in specific regions or catchments.

Other factors, such as antecedent rainfall and baseline conditions (e.g., soil moisture content and organic matter content), may also influence the threshold of erosive rainfall. For instance, antecedent soil moisture has a significant effect on runoff generation and soil loss[53–55]; compared with dry soils, wet soils can exhibit a twofold increase in runoff coefficients and shortened runoff initiation times[56]. Organic matter content governs the stability of soil aggregates[3], and stable aggregates are critical for enhancing soil infiltration capacity and reducing erosion. This study has certain limitations. For example, the availability of key data (such as antecedent rainfall and soil moisture) was limited, and other potentially important factors (e.g., the effects of soil organic matter) were not fully considered. The mechanisms through which these factors influence the thresholds of erosive rainfall will be explored in future studies using more comprehensive spatiotemporal datasets. Moreover, because of limited data availability for the Tianshui region, the influence of land cover types on erosive rainfall thresholds there was not evaluated. Despite these limitations, this study provides novel insights by analyzing the variation of erosive rainfall thresholds with rainfall intensity and developing predictive models of erosive rainfall thresholds under different land cover conditions. Nonetheless, it did not account for alternative approaches or regional heterogeneity. Future research should integrate additional methodologies, address data constraints, and explore broader environmental conditions to enhance threshold accuracy and improve predictions of soil erosion and water loss.

Conclusions

Based on long-term runoff plot observations from farmland, forest land, grassland, and abandoned land in representative regions of the Loess Plateau (Suide, Xifeng, and Tianshui), this study applied an improved regression analysis to determine erosive rainfall thresholds under different erosion grades. The variation of erosive rainfall thresholds with rainfall intensity was analyzed, along with the effects of land cover and soil texture. Furthermore, nonlinear regression analysis was employed to establish predictive models of erosive rainfall thresholds for different land cover types. The results indicate that the rainfall threshold for soil erosion on slopes decreases exponentially with increasing rainfall intensity. The regression models are as follows: forest land, $y = 58.943e^{-1.668x}$ ($R^2 = 0.84$, $n = 23$); grassland, $y = 64.596e^{-2.034x}$ ($R^2 = 0.83$, $n = 23$); abandoned land, $y = 74.809e^{-2.308x}$ ($R^2 = 0.80$, $n = 16$); and farmland, $y = 59.986e^{-1.888x}$ ($R^2 = 0.65$, $n = 20$). Soil texture was identified as a key factor influencing erosive rainfall thresholds, with finer textures associated with lower thresholds on forest land, grassland, and abandoned land, while the rate of decline with rainfall intensity became more gradual. Threshold trends also varied by rainfall intensity and region. In Suide, thresholds followed the order forest land > abandoned land ≈ grassland > farmland when rainfall intensity < 0.4 mm/min, and forest land > abandoned land > grassland > farmland when rainfall intensity > 0.4 mm/min. In Xifeng, thresholds followed the order abandoned land > grassland > forest land > farmland when rainfall intensity < 0.4 mm/min, and forest land > grassland ≈ abandoned land > farmland when rainfall intensity > 0.4 mm/min. Soil texture, land cover type, and rainfall characteristics exert significant influences on the effectiveness of vegetation in controlling runoff and soil erosion. These findings advance the understanding of the role of rainfall characteristics in soil erosion processes and provide a scientific basis for erosion forecasting and soil and water conservation planning.

Data availability

Data available on request due to privacy: the data presented in this study are available on request from the corresponding author.

Received: 21 November 2025; Accepted: 29 January 2026
Published online: 02 February 2026

References

1. Omidvar, E., Hajizadeh, Z. & Ghasemieh, H. Sediment yield, runoff and hydraulic characteristics in straw and rock fragment covers. *Soil Tillage. Res.* **194**, 104324 (2019).
2. Wei, L. et al. Reveal of contributing rainfalls to annual soil erosion and the response of runoff sediment output: A case of zonal yellow soil area. *J. Hydrol.* **652**, 132666 (2025).
3. Yu, Y., Zhao, W., Martinez-Murillo, J. F. & Pereira, P. Loess plateau: from degradation to restoration. *Sci. Total Environ.* **738**, 140206 (2020).
4. Wang, W. Study on the relations between rainfall characte-ristics and loss of soil in loess region. *Bull. Soil Water Conserv.* **02**, 58–63 (1984).
5. Raj, R., Saharia, M., Chakma, S. & Rafieinasab, A. Mapping rainfall erosivity over India using multiple precipitation datasets. *Catena* **214**, 106256 (2022).
6. Zhang, J. et al. Evaluating the hydrological function of vegetation restoration in fragile karst area: insights from the continuous surface and subsurface runoff monitoring. *Soil Tillage. Res.* **234**, 105847 (2023).
7. Renard, K. G., Foster, G. R., Weesies, G. A. & Porter, J. P. Revised universal soil loss equation (Rusle). *J. Soil Water Conserv.* **46** (1), 30–33 (1991).
8. Liao, J. et al. RUSLE tends to overestimate soil erosion in revegetated conditions: evidence from long-term runoff plots monitoring on china's loess plateau. *Catena* **258**, 109285 (2025).
9. Panagos, P. et al. Rainfall erosivity in Europe. *Sci. Total Environ.* **511**, 801–814 (2015).
10. Takhellambam, B. S. et al. Projected mid-century rainfall erosivity under climate change over the southeastern United States. *Sci. Total Environ.* **865**, 161119 (2023).
11. Deng, O., Li, M., Yang, B., Yang, G. & Li, Y. Erosive rainfall thresholds identification using statistical approaches in a karst yellow soil mountain Erosion-Prone region in Southwest China. *Agriculture* **14** (8), 1421 (2024).
12. Jiao, X. et al. Preliminary research on the threshold of erosive rainfall on karst slopes. *J. Soil Water Conserv.* **37** (05), 57–63 (2023).
13. Todisco, F., Vergni, L., Vinci, A. & Pampalone, V. Practical thresholds to distinguish erosive and Rill rainfall events. *J. Hydrol.* **579**, 124173 (2019).
14. Wischmeier, W. H. & Smith, D. D. *Predicting Rainfall Erosion Losses: a Guide To Conservation Planning* (Department of Agriculture, Science and Education Administration, 1978).
15. Wang, W. & Jiao, J. Qutantitative evaluation on factors influencing soil erosion in China. *Bull. Soil Water Conserv.* **05**, 1–20 (1996).
16. Ma, L., Zuo, C. & Qiu, G. Erosive rainfall characteristics on red soil slope land in Northern Jiangxi Province. *Bull. Soil Water Conserv.* **30** (01), 74–79 (2010).
17. Li, L., Wang, Z. & Jiao, J. Erosive rainfall and rainfall erosivity in purple hilly area. *Sci. Soil. Water Conserv.* **11** (01), 8–16 (2013).
18. Jiang, Z. & Li, X. Study on the rainfall erosivity and the topographicfactor of predicting soil loss equation in theloess plateau. *Res. Soil. Water Conserv.* **01**, 40–45 (1988).
19. Yang, Z. S. Study on soil loss equation of cultivated slopeland in Northeast mountain region of Yunnan Province. *Bull. Soil Water Conserv.* **19** (1), 1–9 (1999).
20. Xie, Y., Liu, B. & Nearing, M. A. Practical thresholds for separating erosive and non–erosive storms. *Trans. ASAE*. **45** (6), 1843 (2002).
21. Jin, J., Xie, Y. & Zhang, K. A study on erosive rainfall standards based on different sample sizes. *Bull. Soil Water Conserv.* **02**, 31–33 (2001).
22. Liu, H., Yuan, A. & Lu, B. Study on erosive ranifall standard of Beijing. *Res. Soil. Water Conserv.* **01**, 215–217 (2007).
23. Xia, L., Song, X., Fu, N., Li, H. & Li, Y. Threshold standard of erosive rainfall under different underlying surface conditions in the loess plateau gully region of East Gansu, China. *Adv. Water Sci.* **29** (6), 828–838 (2018).
24. Zhang, W. Y., Wang, B. T., Yang, G. X. & Zhang, K. Erosive rainfall and characteristics analysis of sediment yield on yellow soil area in karst mountainous. *Ecol. Environ. Sci.* **23** (11), 1776–1782 (2014).
25. Li, X., Kong, J. & Gao, Q. Experimental study on threshold rainfall determination for artificial Rainwater-Harvesting catchments. *Adv. Water Sci.* **04**, 516–522 (2001).
26. Huang, J., Wu, P. & Zhao, X. Experimental study on the nonlinear multi-parameter rainfall-runoff threshold model. *J. Beijing For. Univ.* **33** (1), 84–89 (2011).
27. Zhang, Z. et al. Variations in erosive rainfall threshold and sediment production between karst and non-karst slopes. *Catena* **251**, 108820 (2025).
28. Wang, Y., Yang, Y., Liu, B. Y. & Liu, Y. N. Erosive rainfall thresholds for five typical soils in water erosion region of China. *Bull. Soil. Water Conserv.* **42**, 227–233 (2022).
29. Liu, J., Liang, Y., Gao, G., Dunkerley, D. & Fu, B. Quantifying the effects of rainfall intensity fluctuation on runoff and soil loss: from indicators to models. *J. Hydrol.* **607**, 127494 (2022).
30. Yan, Y. et al. Effects of rainfall intensity on runoff and sediment yields on bare slopes in a karst area. *SW China Geoderma*. **330**, 30–40 (2018).
31. Chen, Y. et al. Balancing green and grain trade. *Nat. Geosci.* **8** (10), 739–741 (2015).
32. Wang, S. et al. Reduced sediment transport in the yellow river due to anthropogenic changes. *Nat. Geosci.* **9**, 38–41 (2016).
33. Németová, Z., Kohnová, S. & Sabová, Z. Determining the dependence of a landscape's ecological stability and the intensity of erosion during 1990–2018. *Water*. **16** (3), 378 (2024).
34. Ministry of Water Resources of the People's Republic of China. *Standards for Classification and Gradation of Soil Erosion (SL190-2007)* (China Water and Power, 2008).
35. Li, Y., Han, R. & Wang, Z. Soil water properties and its zonation in the loess plateau. *Res. Soil. Water Conserv.* **1985** (02), 1–17 (1985).
36. Zhao, C., Shao, M. A., Jia, X. & Zhang, C. Particle size distribution of soils (0–500 cm) in the loess Plateau, China. *Geoderma Reg.* **7** (3), 251–258 (2016).
37. Diskin, M. H. Definition and uses of the linear regression model. *Water Resour. Res.* **6** (6), 1668–1673 (1970).
38. Fink, D. H. & Frasier, G. W. Evaluating weathering characteristics of water-harvesting catchments from rainfall-runoff analyses. *Soil Sci. Soc. Am. J.* **41** (3), 618–622 (1977).
39. Fink, D. H., Frasier, G. W. & Myers, L. E., Water harvesting treatment evaluation at granite reef 1. *JAWRA J. Am. Water Resour. Assoc.* **15**(3), 861–873 (1979).
40. Huang, J. et al. Characteristics of slope runoff and sediment yield under individual rainfall events in Southern red soil region. *Sci. Soil. Water Conserv.* **14** (02), 23–30 (2016).

41. Liu, H. et al. Spatial patterns of soil carbon and nutrient distribution during vegetation restoration in red soil regions. *Plant. Soil.* 1–22 (2025).
42. Tang, Y. et al. Vertically oriented roots affect soil water infiltration by decomposition and altering soil structure: an examination based on CT technology and innovation in soil infiltration research methods. *Plant. Soil.* 1–17 (2025).
43. Chen, Z. et al. Utilizing an 11-year runoff plot dataset to evaluate the regulation of six land management practices on runoff and sediment on Mollisols slopes and the applicability of the WEPP model. *Soil Tillage. Res.* **252**, 106601 (2025).
44. Lev-Yadun, S., Katzir, G. & Neeman, G. Rheum palaestinum (desert rhubarb), a self-irrigating desert plant. *Naturwissenschaften* **96** (3), 393–397 (2009).
45. Lann, T. et al. Hydro-mechanical effects of vegetation on slope stability: A review. *Sci. Total Environ.* **926**, 171691 (2024).
46. Moore, E. B. et al. Connections between roots and soil health across agriculture management practices. *Plant Soil.* (2025).
47. Modeste, M., Abdellatif, K., Nadia, M. & Mohamed, S. Effects of land use and cover type on the risks of runoff and water erosion: infiltration tests in the Ourika watershed (High Atlas, Morocco). *Euro-Mediterranean J. Environ. Integr.* **3** (1), 8 (2018).
48. Zhou, P. & Wang, Z. A study on rainstorm causing soil erosion in the loess plateau. *J. Soil Water Conserv.* **03**, 1–5 (1992).
49. Smerdon, E. T. & Beasley, R. P. Critical tractive forces in cohesive soils. *Agric. Eng.* **42** (1), 26–29 (1961).
50. de Almeida, W. S., Seitz, S., de Oliveira, L. F. C. & de Carvalho, D. F. Duration and intensity of rainfall events with the same erosivity change sediment yield and runoff rates. *Int. Soil. Water Conserv. Res.* **9** (1), 69–75 (2021).
51. Zhang, X. K., Xu, J. H., Lu, X. Q., Deng, Y. J. & Gao, D. W. A study on the soil loss equation in Heilongjiang Province. *Bull. Soil Water Conserv.* **12** (4), 1–9 (1992).
52. Tian, X. et al. Study on daily erosive rainfall standard in the Poyang lake basin. *J. Soil Water Conserv.* **35** (03), 185–189 (2021).
53. Nortcliff, S., Ross, S. M. & Thornes, J. B. Soil moisture, runoff and sediment yield from differentially cleared tropical rainforest plots. (1990).
54. Scipal, K., Scheffler, C. & Wagner, W. Soil moisture-runoff relation at the catchment scale as observed with coarse resolution microwave remote sensing. *Hydrol. Earth Syst. Sci.* **9** (3), 173–183 (2005).
55. Zhou, J. et al. Effects of precipitation and restoration vegetation on soil erosion in a semi-arid environment in the loess Plateau, China. *Catena* **137**, 1–11 (2016).
56. Li, X. Y. et al. Controls of infiltration–runoff processes in mediterranean karst rangelands in SE Spain. *Catena* **86** (2), 98–109 (2011).

Acknowledgements
We would like to express our respect and gratitude to the anonymous reviewers and editors for their professional comments and suggestions.

Author contributions
Overall design, Z.H. and S.H.; methodology, G.Y. and S.H.; software, Z.L. and R.W.; formal analysis, D.Q., P.X. and H.T.; data curation, H.D. and Y.G.; writing—original draft preparation, G.Y.; writing—review and editing, Z.H. and L.Z. All authors have read and agreed to the published version of the manuscript.

Funding
The Natural Science Foundation of Henan Province (252300420859); National Natural Science Foundation of China (U2243210); Key Technology Research Project of Water Conservancy Science and Technology of Henan Provincial Water Resources Department (GG202516).

Declarations

Competing interests
The authors declare no competing interests.

Additional information
Correspondence and requests for materials should be addressed to S.H.

Reprints and permissions information is available at www.nature.com/reprints.

Publisher's note Springer Nature remains neutral with regard to jurisdictional claims in published maps and institutional affiliations.

Open Access This article is licensed under a Creative Commons Attribution-NonCommercial-NoDerivatives 4.0 International License, which permits any non-commercial use, sharing, distribution and reproduction in any medium or format, as long as you give appropriate credit to the original author(s) and the source, provide a link to the Creative Commons licence, and indicate if you modified the licensed material. You do not have permission under this licence to share adapted material derived from this article or parts of it. The images or other third party material in this article are included in the article's Creative Commons licence, unless indicated otherwise in a credit line to the material. If material is not included in the article's Creative Commons licence and your intended use is not permitted by statutory regulation or exceeds the permitted use, you will need to obtain permission directly from the copyright holder. To view a copy of this licence, visit http://creativecommons.org/licenses/by-nc-nd/4.0/.

© The Author(s) 2026